molecules

MDPI

Communication

CO_2 Capture Mechanism by Deep Eutectic Solvents Formed by Choline Prolinate and Ethylene Glycol

Mingzhe Chen and Jinming Xu *

School of Science, China University of Geosciences, Beijing 100083, China; 2019220039@email.cugb.edu.cn
* Correspondence: xujm@cugb.edu.cn

Abstract: The choline prolinate ([Ch][Pro]) as a hydrogen bond acceptor and ethylene glycol (EG) as a hydrogen bond donor are both used to synthesize the deep eutectic solvents (DESs) [Ch][Pro]-EG to capture CO_2. The CO_2 capacity of [Ch][Pro]-EG is determined, and the nuclear magnetic resonance (NMR) and infrared (IR) spectrum are used to investigate the CO_2 capture mechanism. The results indicate that CO_2 reacts with both the amino group of $[Pro]^-$ anion and the hydroxyl group of EG, and the mechanism found in this work is different from that reported in the literature for the [Ch][Pro]-EG DESs.

Keywords: CO_2 capture; absorption; deep eutectic solvents; mechanism; proline

1. Introduction

Carbon dioxide (CO_2) emissions have increased at an unbelievable rate, which causes great concern in global society and results in increasing atmospheric temperature and rising sea levels. The unprecedented amounts of atmospheric CO_2 are mainly emitted from the combustion of fossil fuels in industry [1–3]. An urgent demand to reduce the rising levels of CO_2 has driven different industries and fields to explore efficient CO_2 capture technologies. The current prominent commercial method for CO_2 capture in the industry is the alkanolamine-based scrubbing process, which mainly utilizes aqueous solutions of alkanolamines to absorb CO_2 chemically [4,5]. However, alkanolamine-based sorption systems have several inherent drawbacks, such as solvent degradations, equipment corrosion, and high absorbent regeneration energy [6,7]. Thus, developing new efficient sorption systems capable of avoiding the above-mentioned drawbacks is one of the main challenges in the field of carbon capture and storage [8].

In the past decades, as an alternative to amine-based absorbents, ionic liquids (ILs) have received a lot of attention in the CO_2 capture field because of their attractive properties, including negligible vapor pressure, high thermal and chemical stability, low flammability, and tunable structures [9,10]. To date, a number of functionalized ILs, which can chemically capture CO_2, have been investigated for CO_2 capture. Among them, anion-functionalized ILs, such as azolide-based and amine-based ILs, exhibit high CO_2 absorption capacities [11–13]. However, the main shortcoming of the functionalized ILs is their high viscosity, which limits their large-scale industrial application.

In recent years, deep eutectic solvents (DESs), emerging as a new kind of solvent, have gained significant attention because they share many features with ILs, such as very low vapor pressure and tunable properties [14,15]. At present, most DESs are formed by combining hydrogen bond donors (HBDs) and hydrogen bond acceptors (HBAs), and the intermolecular hydrogen bonds formed between HBDs and HBAs induce a large depression of melting or freezing temperatures of DESs [16,17]. Due to their attractive properties, DESs have been widely investigated in many fields, including organic synthesis, catalysis, biodiesel conversion, electrochemistry, and nanotechnology [18–23].

Moreover, the applications of DESs to capture CO_2 have also been widely studied [24,25]. Many DESs formed by halide anion-based quaternary ammonium/phosphonium salts with

Citation: Chen, M.; Xu, J. CO_2 Capture Mechanism by Deep Eutectic Solvents Formed by Choline Prolinate and Ethylene Glycol. *Molecules* **2023**, *28*, 5461. https://doi.org/10.3390/molecules28145461

Academic Editors: Iuliia V. Voroshylova and Elisabete Ferreira

Received: 8 June 2023
Revised: 12 July 2023
Accepted: 13 July 2023
Published: 17 July 2023

common HBDs (ethylene glycol, glycerol, lactic acid, decanoic acid, acetic acid, urea, etc.) have been utilized to capture CO_2, and these DESs exhibit low CO_2 capacities because they physically interact with CO_2 [26–31]. In order to improve the CO_2 capacity of DESs, several works introduce amino groups into the components (HBDs or HBAs) of DESs. These amino-contained DESs, which are amino-functionalized DESs, present a high capacity due to the chemical interactions between amino groups and CO_2 [32–37]. Zhang et al. reported the anime-functionalized DESs composed of 1-butyl-3-methylimidazolium chloride (BmimCl) and monoethanolamine (MEA) for CO_2 capture [32], and results indicated that CO_2 reacted with the amino group of MEA by forming a carbamate species and BmimCl:MEA (1:4, molar ratio) exhibited a high CO_2 capacity (21.4 wt%) at 25 °C and 100 kPa. Trivedi and co-authors studied CO_2 capture by DESs formed by monoethanolammonium chloride ([MEAH][Cl]) and ethylenediamine (EDA), and the DESs [MEAH][Cl]-EDA also exhibited a high capacity through the reaction between CO_2 and EDA. [33] Shukla et al. investigated CO_2 absorption by DESs composed of ammonium salts-based HBAs (choline chloride (ChCl), tetrabutylammonium bromide (TBAB), etc.) and amine-based HBDs (MEA, EDA, tetraethylenepentamine (TEPA), etc.), finding that the synergistic interactions between HBAs and HBDs were important factors for CO_2 capture by DESs [34]. Wu and co-authors synthesized DESs comprising triethylenetetrammonium chloride ([TETAH][Cl]) and EG or diethylene glycol (DG), and [TETAH][Cl]:EG(1:3) could absorb CO_2 up to 17.5 wt% at 1 atm and 40 °C [35]. Then, hydrophobic amine-functionalized DESs were developed for carbon capture. The hydrophobic DESs [TETAH][Cl]: Thymol (1:3) could chemically capture CO_2 through the reaction between CO_2 and the free amino groups on the cation $[TETAH]^+$ [36].

Functionalized DESs containing basic anions in the solvents are also proposed to capture carbon. It is found that anion-functionalized DESs, consisting of EG and solid azolide ILs (tetraethylphosphonium imidazolide ($[P_{2222}][Im]$), tetraethylphosphonium 1,2,4-triazolide ($[P_{2222}][Triz]$), etc.), could chemically absorb CO_2 through the reaction between CO_2 and EG [38]. Interestingly, CO_2 absorption behaviors of anion-functionalized DESs based on 1,2,3-triazole (Tz) can be changed by tuning the strength of hydrogen bonds formed between the anion $[Tz]^-$ and HBDs (EG or Tz) [39]. The DESs composed of 1-ethyl-3-methylimidazolium 2-cyanopyrrolide ([Emim][2-CNpyr]) and EG can also chemically capture CO_2, and CO_2 can react with both [Emim][2-CNpyr] and EG [40]. The CO_2 absorption by phenol-derived anion-functionalized DESs was also studied [41], and the results indicated that the steric hindrance of functional groups of HBDs greatly impacted the absorption mechanisms. For example, when CO_2 was captured by $[Et_4N][Car]$-EG ($[Et_4N][Car]$: tetraethylammonium carvacrolate), CO_2 reacted with both the anion $[Car]^-$ and EG. Nevertheless, for the $[Et_4N][Car]$-$4CH_3$-Im ($4CH_3$-Im: 4-methylimidazole) system, CO_2 reacted with the anion $[Car]^-$, but did not react with $4CH_3$-Im. In addition, superbase-derived anion-functionalized DESs were also explored for CO_2 capture, such as [DBUH][Im]-EG (DBU: 1,8-diazabicyclo-[5,4,0]undec-7-ene) [42], [DBUH][MLU]-EG (MLU: methyl urea) [43], [DBNH][Triz]-EG (DBN: 1,5-Diazabicyclo[4.3.0]non-5-ene) [44], [DBUH][Car]-EG [45], DBN-EU (EU: 2-imidazolidone) [46], [DBUH][4-F-PhO]-EG(4-F-PhO:4-Fluorophenolate) [47], ternary DESs [DBUH][4-F-PhO]-4-F-PhOH-EG [47], and DBN-BmimCl-Im [48]. According to the results reported in the literature, it can be found that the components of DESs greatly affect the CO_2 absorption behaviors of functionalized DESs. Therefore, revealing the interactions between CO_2 and the components of DESs is of great importance to the design of efficient DESs [49].

Recently, the amino-functionalized DESs, consisting of choline prolinate ([Ch][Pro]) and EG, were prepared to capture CO_2, and the mechanism studies suggested that CO_2 reacted with the anion $[Pro]^-$, forming carbamate acid, but not with EG [50] (Scheme 1). In this work, we also investigate the CO_2 capture mechanism by [Ch][Pro]-EG DESs. However, based on the nuclear magnetic resonance (NMR) and Fourier transform infrared (FTIR) results, we find that CO_2 can react with both the anion $[Pro]^-$ and EG (Scheme 1), and the discussion can be found in the sections below.

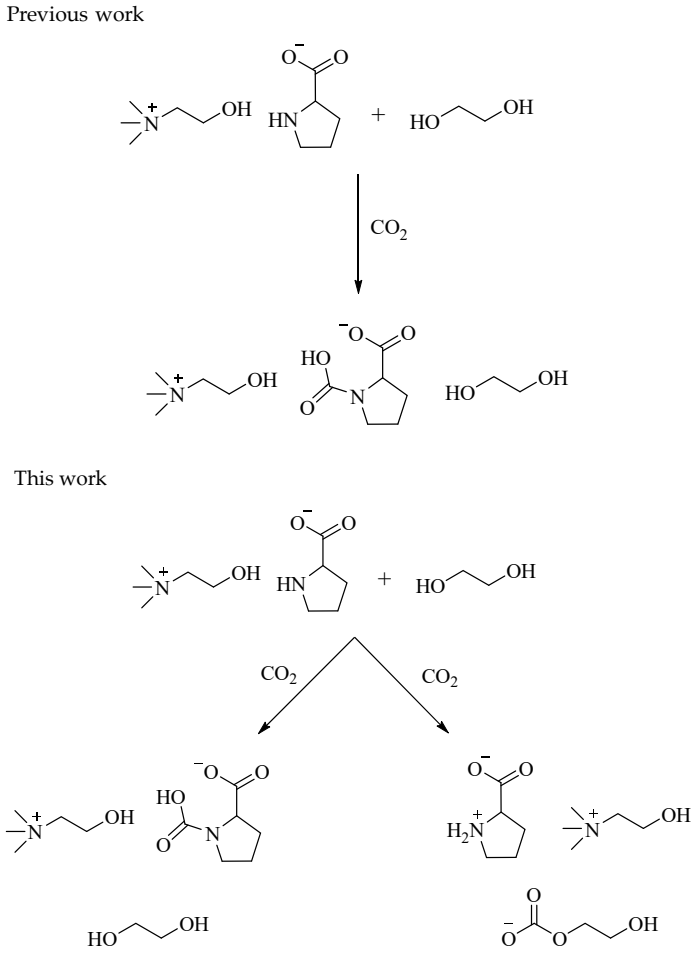

Scheme 1. The CO_2 capture mechanism by [Ch][Pro]-EG reported in previous work [50] and found in this work.

2. Results and Discussion

The CO_2 capacities of [Ch][Pro]-EG solvents are determined at 25 °C and 1.0 atm (Figure 1). As seen in Figure 1, [Ch][Pro]:EG (1:3, molar ratio), (1:4), and (1:5) could capture 0.66, 0.67, and 0.71 mol CO_2/mol DESs, respectively.

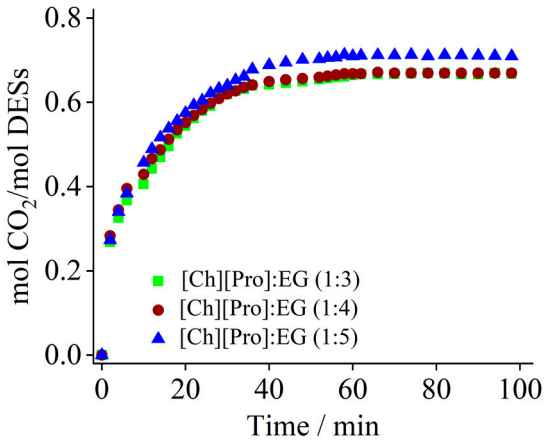

Figure 1. The CO_2 capture by [Ch][Pro]-EG DESs at 25 °C and 1.0 atm.

Then, NMR and FTIR methods are utilized to study the interactions between CO_2 and solvents. The ^{13}C NMR spectra of [Ch][Pro]:EG (1:3) before and after CO_2 capture are presented in Figure 2a. After CO_2 capture, new peaks can be observed at 159.7 (C-f),

157.8 (C-4), and 66.4 (C-3) ppm, and the signal of C-d carbon of the anion $[Pro]^-$ shifts upward from 62.2 to 61.1 ppm. The new peak at 159.7 ppm is ascribed to the carbonyl carbon of carbamate acid, suggesting the CO_2 reacts with the anion $[Pro]^-$ [50]. The new peaks at 157.8 ppm can be attributed to the carbonyl carbon of the carbonate species formed by the reaction between CO_2 and EG [39,42,43]. The peak at 66.4 ppm is the methylene carbon of the carbonate species derived from EG. The other methylene carbon (C-2) peak of carbonate is overlapped with the C-d carbon (61.1 ppm). The NMR results of [Ch][Pro]:EG (1:4) and (1:5) show a similar phenomenon, and the NMR spectra of [Ch][Pro]:EG (1:5) before and after CO_2 capture are shown in Figure 2b. The new peaks after capture are at 159.2 (C-f), 157.6 (C-4), and 66.2 (C-3) ppm for [Ch][Pro]:EG (1:5), indicating again that CO_2 reacts with both the anion $[Pro]^-$ and EG.

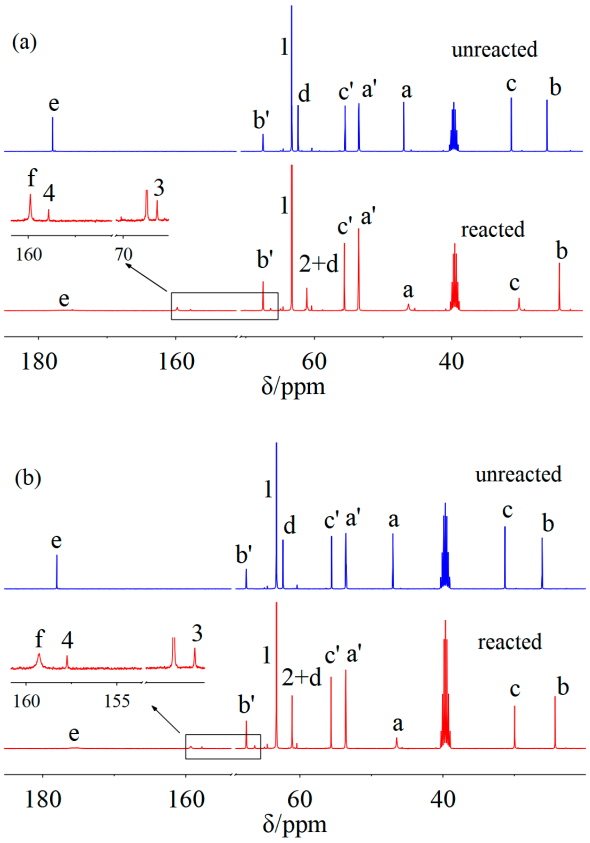

Figure 2. The ^{13}C NMR spectra of [Ch][Pro]:EG (1:3) (**a**) and [Ch][Pro]:EG (1:5) (**b**) before and after CO_2 capture. Letters from a to e are the labels of carbon atoms of the $[Pro]^-$ anion with and without CO_2. Letter f is the carbonyl carbon attached to the N atom of $[Pro]^-$ anion. Letters from a′ to c′ are the lables of carbon atoms of the cation $[Ch]^+$. Numer 1 is the carbon atom of EG. Numbers 2–4 are the carbon atoms of EG-based carbonates.

The ^{13}C NMR spectra of [Ch][Pro]:EG (1:2) before and after absorption are also analyzed. As presented in Figure 3a, it can be seen that there are new peaks at 159.6 (C-f), 157.3 (C-4), and 66.0 (C-3) ppm after capture, confirming that CO_2 reacts with EG in the [Ch][Pro]:EG (1:2), which is different from the results reported by Klemm et al. [50]. Furthermore, the ^{13}C NMR spectra of $[Et_4N][Pro]$:EG (1:3) ($[Et_4N][Pro]$: tetraethylammonium prolinate) are also recorded to test whether CO_2 can react with EG after changing cations of DESs. As shown in Figure 3b, four new peaks can be found at 159.5 (C-f), 157.4 (C-4), 66.0 (C-3), and 61.1 (C-2) ppm after capture, suggesting CO_2 can also react with both the anion $[Pro]^-$ and EG in the $[Et_4N][Pro]$:EG (1:3) solvent, which is consistent with the [Ch][Pro]-EG DESs. Fortunately, the C-2 peak ascribed to one of the methylene carbons of EG-based carbonate species can be observed (Figure 3b), and it is not overlapped with C-d

carbon this time. The full-window ^{13}C NMR spectra of the solvents used in this work are shown in Figures S1–S5.

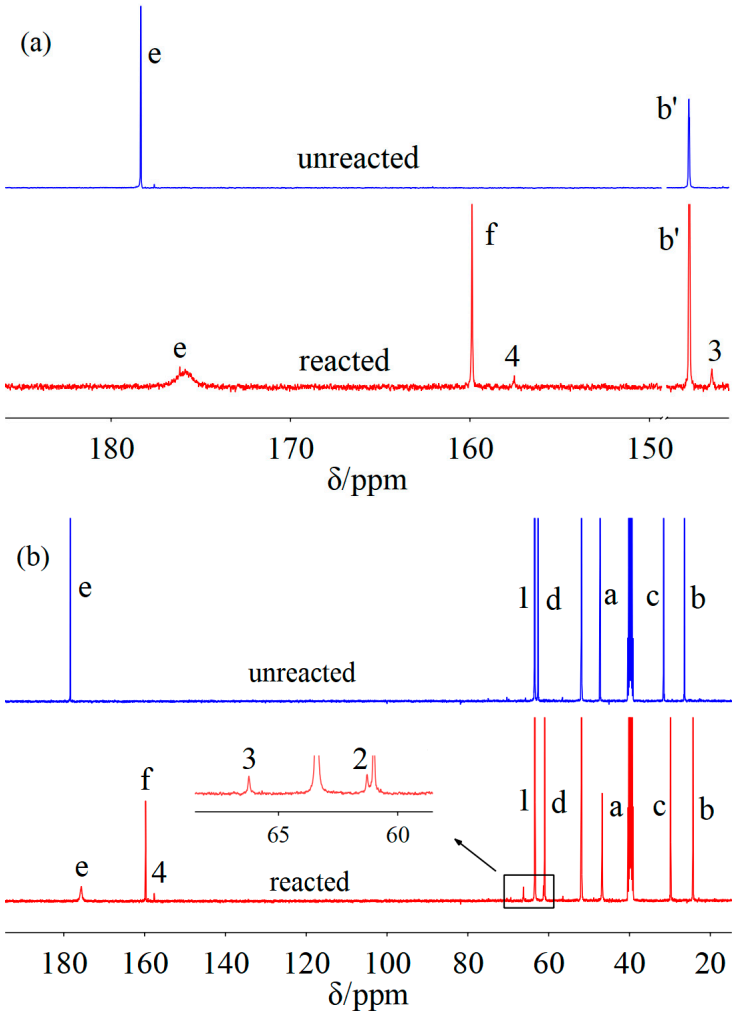

Figure 3. The ^{13}C NMR spectra of [Ch][Pro]:EG (1:2) (**a**) and [Et_4N][Pro]:EG (1:3) (**b**) before and after CO_2 capture. Letters from a to e are the labels of carbon atoms of the $[Pro]^-$ anion with and without CO_2. Letter f is the carbonyl carbon attached to the N atom of $[Pro]^-$ anion. Numer 1 is the carbon atom of EG. Numbers 2–4 are the carbon atoms of EG-based carbonate.

The ^1H NMR spectra of the solvents used before and after CO_2 capture are presented in Figures S6–S10. As can be seen in the ^1H NMR spectra of the DESs after CO_2 capture, the methylene hydrogen (H-3) of EG-based carbonate can be observed. Based on the H-3 peak integral values, the amount of CO_2 captured by EG can be calculated. The loadings of EG-bonded CO_2 of [Ch][Pro]:EG (1:2), (1:3), (1:4), and (1:5) are 0.07(11.3%), 0.10 (15.2%), 0.13 (19.4%), and 0.14 (19.7%) mol CO_2/mol DESs, respectively. The values in parenthesis are the percentages of EG-bonded CO_2 to the overall CO_2 capacity. The results indicate that EG-bonded CO_2 rise with increasing the amount of EG in the DESs. The results reported by reference [50] claimed that CO_2 did not react with EG in the DESs [Ch][Pro]:EG (1:2), probably because the intensities of the H and C peaks of EG-based carbonate in NMR spectra were very weak and these peaks can be easily overlooked if they are not carefully identified.

The FTIR spectra of the DESs used before and after CO_2 capture are shown in Figure 4. As seen in Figure 4a, two new bands at 1623 and 1295 cm^{-1} can be found after absorption for [Ch][Pro]:EG (1:3) system. The band at 1623 cm^{-1} is the combined peak of C=O stretching from the carbamate acid and the carbonate species [40,51–53]. The band at 1295 cm^{-1} can

be attributed to the stretching of the O-COO$^-$ bond [39,40]. Similarly, for the [Ch][Pro]:EG (1:5) system, the new peaks appear at 1627 and 1292 cm^{-1} after CO_2 capture (Figure 4b). Similar peaks can also be observed at 1623 and 1292 cm^{-1} for the solvent [Ch][Pro]:EG (1:2) after capture (Figure 4c). Moreover, two new bands at 1626 and 1289 cm^{-1} can be found as well in the FTIR spectra of [Et$_4$N][Pro]:EG (1:3) after CO_2 absorption (Figure 4d). Therefore, the FTIR results also provide evidence that CO_2 reacts both with the anion [Pro]$^-$ and EG. The full-window FTIR spectra of the solvents before and after CO_2 capture are shown in Figures S11–S15.

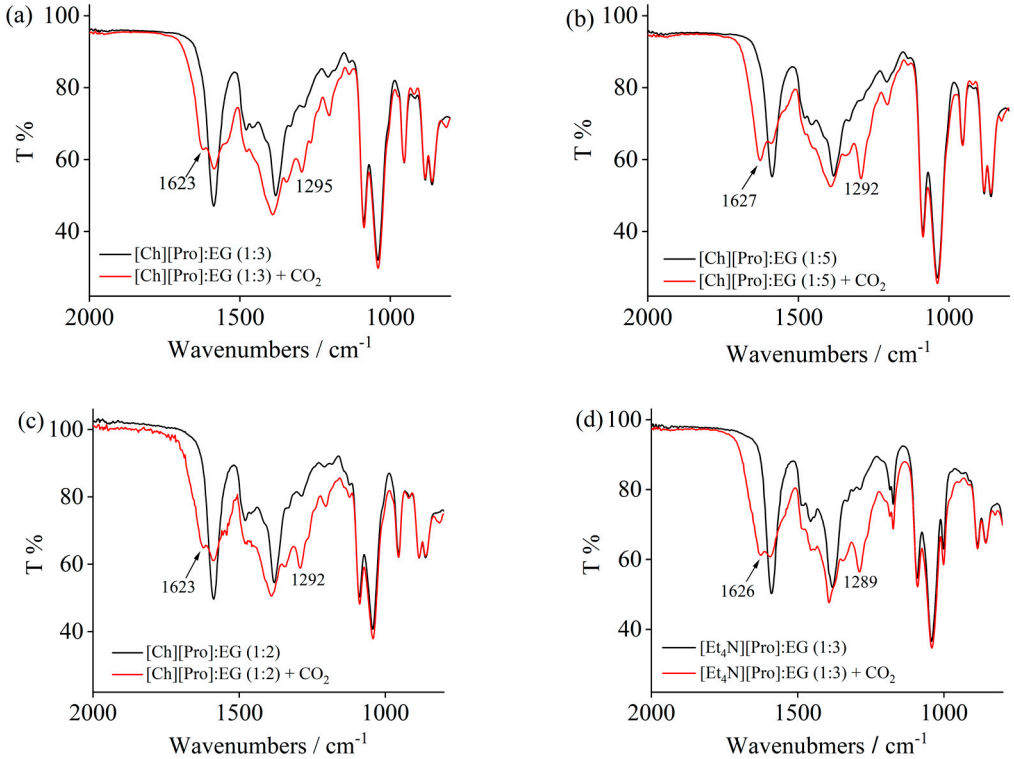

Figure 4. FTIR spectra of [Ch][Pro]:EG (1:3) (**a**), [Ch][Pro]:EG (1:5) (**b**), [Ch][Pro]:EG (1:2) (**c**), and [Et$_4$N][Pro]:EG (1:3) (**d**) before and after CO_2 absorption.

On the basis of the above findings, the possible reaction mechanism between CO_2 and [Ch][Pro]-EG studied is presented in Scheme 2. In the [Ch][Pro]-EG solvent, there is an acid-based reaction between anion [Pro]$^-$ and EG, producing the anion HO–CH$_2$–CH$_2$–O$^-$. The amino group of anion [Pro]$^-$ may influence the acidity of EG through the interaction between the N atom of an amino group and the H atom of the -OH group, so EG can be deprotonated.

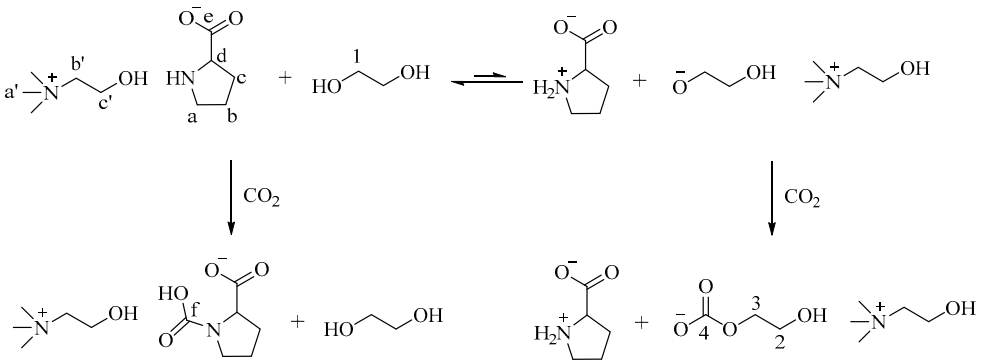

Scheme 2. The possible CO_2 capture mechanism by [Ch][Pro]-EG used in this work.

When CO_2 is absorbed by [Ch][Pro]-EG solvent, CO_2 can react with $[Pro]^-$ to form a carbamate acid, and it can also react with $HO–CH_2–CH_2–O^-$ to form carbonate species.

3. Materials and Methods

3.1. Materials and Characterizations

Proline (99%) and ethylene glycol (99.5%) were obtained from J&K Scientific Ltd. (Beijing, China) Choline hydroxide ([Ch][OH], 44% *w*/*w* in water) and tetramethylammonium hydroxide ($[Et_4N][OH]$) (25% *w*/*w* in water) were purchased from Innochem Science and Technology Co., Ltd. (Beijing, China). CO_2 (≥99.99%) was provided by Beijing ZG Special Gases Sci. and Tech. Co. Ltd. (Beijing, China).

The ^{13}C NMR spectra were taken on a Bruker spectrometer (151 MHz) using d_6-DMSO as the internal reference. The FTIR spectra were recorded on a Perkin-Elmer frontier spectrometer equipped with an attenuated total reflection (ATR) accessory. Ethylene glycol was dried with 4 Å molecular sieve prior to use. The exact concentrations of [Ch][OH] and $[Et_4N][OH]$ in aqueous solution were titrated with potassium hydrogen phthalate (KHP). The water content in the solvents was determined by Karl–Fischer titration method.

3.2. Synthesis of Proline-Based ILs

For the synthesis of [Ch][Pro], equimolar proline (Pro) was added to the aqueous solution of [Ch][OH] ([Ch][OH]:Pro = 1:1). The mixture was stirred at room temperature for 2 h, and then water in the solution was removed by using rotary evaporation at 70 °C to obtain the IL [Ch][Pro]. Finally, the IL [Ch][Pro] was dried under vacuum at 70 °C prior to use.

The synthesis of $[Et_4N][Pro]$ was similar to that of [Ch][Pro].

3.3. Synthesis of DESs

For the DESs [Ch][Pro]-EG, the IL [Cho][Pro] and ethylene glycol were mixed at desired molar ratios, and then the mixtures were stirred at 70 °C until homogenous liquids were formed, and then liquid solvents were cooled down to room temperature to obtain the DESs. The water contents of the DESs [Ch][Pro]:EG (1:2), (1:3), (1:4), and (1:5) were 0.21, 0.18, 0.17, and 0.17 wt%, respectively.

The synthesis of the solvent $[Et_4N][Pro]$:EG (1:3) was similar to those of [Ch][Pro]-EG DESs.

NMR and FTIR data of solvents used in this work:

[Ch][Pro]:EG (1:2): ^{13}C NMR (151 MHz, d_6-DMSO) δ = 178.2, 67.4, 63.2, 62.4, 55.4, 53.4, 47.0, 31.3, 26.1 ppm. FTIR: ν = 3282, 2920, 2866, 1587, 1480, 1378, 1089, 1037, 958, 885, 863, 635 cm^{-1}.

[Ch][Pro]:EG (1:3): ^{13}C NMR (151 MHz, d_6-DMSO) δ = 177.8, 67.3, 63.2, 62.2, 55.4, 53.4, 46.8, 31.1, 26.0 ppm. FTIR: ν = 3283, 2924, 2872, 1587, 1480, 1381, 1086, 1039, 954, 884, 861, 627 cm^{-1}.

[Ch][Pro]:EG (1:4): ^{13}C NMR (151 MHz, d_6-DMSO) δ = 178.4, 67.5, 63.2, 62.4, 55.5, 53.5, 46.9, 31.3, 26.1 ppm. FTIR: ν = 3285, 2928, 2870, 1587, 1480, 1382, 1087, 1039, 953, 883, 861, 624 cm^{-1}.

[Ch][Pro]:EG (1:5): ^{13}C NMR (151 MHz, d_6-DMSO) δ = 177.9, 67.3, 63.1, 62.2, 55.4, 53.4, 46.8, 31.3, 26.0 ppm. FTIR: ν = 3290, 2932, 2864, 1587, 1480, 1382, 1087, 1038, 954, 884, 861, 623 cm^{-1}.

$[Et_4N][Pro]$:EG (1:3): ^{13}C NMR (151 MHz, d_6-DMSO) δ = 178.1, 63.2, 62.4, 51.6, 47.1, 31.3, 26.1, 7.1 ppm. FTIR: ν = 3285, 2922, 2869, 1588, 1457, 1382, 1175, 1092, 1043, 1002, 884, 855, 784, 636 cm^{-1}.

3.4. Absorption of CO_2

DESs (~2 g) were added into a glass tube with an inner diameter of 10 mm. CO_2 (~50 mL/min) was bubbled into the glass tube, which was partially immersed in a water bath at the required temperature. The amount of CO_2 absorbed by solvents can be calcu-

lated by the weights of the tube before and after CO_2 absorption, which were determined by an electronic balance with an accuracy of ±0.1 mg. The weight of the tube was measured at regular intervals during the absorption process. If the weight of the tube did not change with time, the CO_2 absorption by DESs was considered to have reached saturation.

4. Conclusions

The CO_2 capture mechanism by DESs consisting of [Ch][Pro] and EG is studied by using NMR and FTIR methods. The NMR and FTIR results reveal that CO_2 can react with both the anion $[Pro]^-$ and EG. In the solvents, EG can be deprotonated by the amino group of the anion $[Pro]^-$, resulting in the formation of the anion $HO–CH_2—CH_2–O^-$. During the absorption process, CO_2 can react both with the amino group of the anion $[Pro]^-$ and the O^- of the anion $HO–CH_2–CH_2–O^-$, forming carbamate acid and carbonate species, respectively. For the $[Et_4N]$[Pro]:EG (1:3) solvent, CO_2 can also react with both the anion $[Pro]^-$ and EG. We think the findings of this work will be useful for understanding the interactions between CO_2 and the components of DESs.

Supplementary Materials: The following supporting information can be downloaded at: https://www.mdpi.com/article/10.3390/molecules28145461/s1, Figure S1: The ^{13}C NMR spectra of [Ch][Pro]:EG (1:3) before (a) and after (b) CO_2 capture.; Figure S2: The ^{13}C NMR spectra of [Ch][Pro]:EG (1:4) before (a) and after (b) CO_2 capture.; Figure S3: The ^{13}C NMR spectra of [Ch][Pro]:EG (1:5) before (a) and after (b) CO_2 capture.; Figure S4: The ^{13}C NMR spectra of [Ch][Pro]:EG (1:2) before (a) and after (b) CO_2 capture.; Figure S5: The ^{13}C NMR spectra of $[Et_4N]$[Pro]:EG (1:3) before (a) and after (b) CO_2 capture.; Figure S6: The ^1H NMR spectra of [Ch][Pro]:EG (1:3) before (a) and after (b) CO_2 capture.; Figure S7: The ^1H NMR spectra of [Ch][Pro]:EG (1:4) before (a) and after (b) CO_2 capture.; Figure S8: The ^1H NMR spectra of [Ch][Pro]:EG (1:5) before (a) and after (b) CO_2 capture.; Figure S9: The ^1H NMR spectra of [Ch][Pro]:EG (1:2) before (a) and after (b) CO_2 capture.; Figure S10: The ^1H NMR spectra of $[Et_4N]$[Pro]:EG (1:3) before (a) and after (b) CO_2 capture.; Figure S11: The FTIR spectra of [Ch][Pro]:EG (1:3) before and after CO_2 capture.; Figure S12: The FTIR spectra of [Ch][Pro]:EG (1:4) before and after CO_2 capture.; Figure S13: The FTIR spectra of [Ch][Pro]:EG (1:5) before and after CO_2 capture.; Figure S14: The FTIR spectra of [Ch][Pro]:EG (1:2) before and after CO_2 capture.; Figure S15: The FTIR spectra of $[Et_4N]$[Pro]:EG (1:3) before and after CO_2 capture.

Author Contributions: Conceptualization, J.X.; methodology, M.C. and J.X.; investigation, M.C. and J.X.; data curation, M.C.; writing—original draft preparation, M.C. and J.X.; supervision, J.X. All authors have read and agreed to the published version of the manuscript.

Funding: This research was funded by the Fundamental Research Funds for the Central Universities, grant number 2652019111.

Data Availability Statement: The data are available on request.

Acknowledgments: The authors thank the instruments and equipment sharing platform of China University of Geosciences (Beijing).

Conflicts of Interest: The authors declare no conflict of interest.

Sample Availability: Not applicable.

References

1. Raganati, F.; Miccio, F.; Ammendola, P. Adsorption of Carbon Dioxide for Post-combustion Capture: A Review. *Energy Fuels* **2021**, *35*, 12845–12868. [CrossRef]
2. Omodolor, I.S.; Otor, H.O.; Andonegui, J.A.; Allen, B.J.; Alba-Rubio, A.C. Dual-Function Materials for CO_2 Capture and Conversion: A Review. *Ind. Eng. Chem. Res.* **2020**, *59*, 17612–17631. [CrossRef]
3. Gao, W.; Liang, S.; Wang, R.; Jiang, Q.; Zhang, Y.; Zheng, Q.; Xie, B.; Toe, C.Y.; Zhu, X.; Wang, J.; et al. Industrial carbon dioxide capture and utilization: State of the art and future challenges. *Chem. Soc. Rev.* **2020**, *49*, 8584–8686. [CrossRef] [PubMed]
4. Langie, K.M.G.; Tak, K.; Kim, C.; Lee, H.W.; Park, K.; Kim, D.; Jung, W.; Lee, C.W.; Oh, H.-S.; Lee, D.K.; et al. Toward economical application of carbon capture and utilization technology with near-zero carbon emission. *Nat. Commun.* **2022**, *13*, 7482. [CrossRef]
5. Aghel, B.; Janati, S.; Wongwises, S.; Shadloo, M.S. Review on CO_2 capture by blended amine solutions. *Int. J. Greenh. Gas Control* **2022**, *119*, 103715. [CrossRef]

6. Kostyanaya, M.I.; Yushkin, A.A.; Bakhtin, D.S.; Legkov, S.A.; Bazhenov, S.D. Perstraction of Heat-Stable Salts from Aqueous Alkanolamine Solutions. *Pet. Chem.* **2022**, *62*, 1254–1266. [CrossRef]
7. Zhao, F.; Cui, C.; Dong, S.; Xu, X.; Liu, H. An overview on the corrosion mechanisms and inhibition techniques for amine-based post-combustion carbon capture process. *Sep. Purif. Technol.* **2023**, *304*, 122091. [CrossRef]
8. Siegel, R.E.; Pattanayak, S.; Berben, L.A. Reactive Capture of CO_2: Opportunities and Challenges. *ACS Catal.* **2023**, *13*, 766–784. [CrossRef]
9. Zeng, S.; Zhang, X.; Bai, L.; Zhang, X.; Wang, H.; Wang, J.; Bao, D.; Li, M.; Liu, X.; Zhang, S. Ionic-Liquid-Based CO_2 Capture Systems: Structure, Interaction and Process. *Chem. Rev.* **2017**, *117*, 9625–9673. [CrossRef]
10. Sheridan, Q.R.; Schneider, W.F.; Maginn, E.J. Role of Molecular Modeling in the Development of CO_2–Reactive Ionic Liquids. *Chem. Rev.* **2018**, *118*, 5242–5260. [CrossRef]
11. Aghaie, M.; Rezaei, N.; Zendehboudi, S. A systematic review on CO_2 capture with ionic liquids: Current status and future prospects. *Renew. Sustain. Energy Rev.* **2018**, *96*, 502–525. [CrossRef]
12. Chen, F.-F.; Huang, K.; Zhou, Y.; Tian, Z.-Q.; Zhu, X.; Tao, D.-J.; Jiang, D.-E.; Dai, S. Multi-Molar Absorption of CO_2 by the Activation of Carboxylate Groups in Amino Acid Ionic Liquids. *Angew. Chem. Int. Ed.* **2016**, *55*, 7166–7170. [CrossRef] [PubMed]
13. Shama, V.M.; Swami, A.R.; Aniruddha, R.; Sreedhar, I.; Reddy, B.M. Process and engineering aspects of carbon capture by ionic liquids. *J. CO_2 Util.* **2021**, *48*, 101507. [CrossRef]
14. Yu, D.; Xue, Z.; Mu, T. Deep eutectic solvents as a green toolbox for synthesis. *Cell Rep. Phys. Sci.* **2022**, *3*, 100809. [CrossRef]
15. El Achkar, T.; Greige-Gerges, H.; Fourmentin, S. Basics and properties of deep eutectic solvents: A review. *Environ. Chem. Lett.* **2021**, *19*, 3397–3408. [CrossRef]
16. Wu, J.; Liang, Q.; Yu, X.; Lü, Q.-F.; Ma, L.; Qin, X.; Chen, G.; Li, B. Deep Eutectic Solvents for Boosting Electrochemical Energy Storage and Conversion: A Review and Perspective. *Adv. Funct. Mater.* **2021**, *31*, 2011102. [CrossRef]
17. Omar, K.A.; Sadeghi, R. Physicochemical properties of deep eutectic solvents: A review. *J. Mol. Liq.* **2022**, *360*, 119524. [CrossRef]
18. Hansen, B.B.; Spittle, S.; Chen, B.; Poe, D.; Zhang, Y.; Klein, J.M.; Horton, A.; Adhikari, L.; Zelovich, T.; Doherty, B.W.; et al. Deep Eutectic Solvents: A Review of Fundamentals and Applications. *Chem. Rev.* **2021**, *121*, 1232–1285. [CrossRef]
19. Yu, D.; Xue, Z.; Mu, T. Eutectics: Formation, properties, and applications. *Chem. Soc. Rev.* **2021**, *50*, 8596–8638. [CrossRef]
20. Zhang, H.; Vicent-Luna, J.M.; Tao, S.; Calero, S.; Jiménez Riobóo, R.J.; Ferrer, M.L.; del Monte, F.; Gutiérrez, M.C. Transitioning from Ionic Liquids to Deep Eutectic Solvents. *ACS Sustain. Chem. Eng.* **2022**, *10*, 1232–1245. [CrossRef]
21. Skowrońska, D.; Wilpiszewska, K. Deep Eutectic Solvents for Starch Treatment. *Polymers* **2022**, *14*, 220. [CrossRef] [PubMed]
22. Tao, D.-J.; Qu, F.; Li, Z.-M.; Zhou, Y. Promoted absorption of CO at high temperature by cuprous-based ternary deep eutectic solvents. *AIChE J.* **2021**, *67*, e17106. [CrossRef]
23. Xu, G.; Shi, M.; Zhang, P.; Tu, Z.; Hu, X.; Zhang, X.; Wu, Y. Tuning the composition of deep eutectic solvents consisting of tetrabutylammonium chloride and n-decanoic acid for adjustable separation of ethylene and ethane. *Sep. Purif. Technol.* **2022**, *298*, 121680. [CrossRef]
24. Liu, Y.; Dai, Z.; Zhang, Z.; Zeng, S.; Li, F.; Zhang, X.; Nie, Y.; Zhang, L.; Zhang, S.; Ji, X. Ionic liquids/deep eutectic solvents for CO_2 capture: Reviewing and evaluating. *Green Energy Environ.* **2021**, *6*, 314–328. [CrossRef]
25. Xu, Y.; Zhang, R.; Zhou, Y.; Hu, D.; Ge, C.; Fan, W.; Chen, B.; Chen, Y.; Zhang, W.; Liu, H.; et al. Tuning ionic liquid-based functional deep eutectic solvents and other functional mixtures for CO_2 capture. *Chem. Eng. J.* **2023**, *463*, 142298. [CrossRef]
26. Francisco, M.; van den Bruinhorst, A.; Zubeir, L.F.; Peters, C.J.; Kroon, M.C. A new low transition temperature mixture (LTTM) formed by choline chloride + lactic acid: Characterization as solvent for CO_2 capture. *Fluid Phase Equilib.* **2013**, *340*, 77–84. [CrossRef]
27. Leron, R.B.; Caparanga, A.; Li, M.-H. Carbon dioxide solubility in a deep eutectic solvent based on choline chloride and urea at T = 303.15–343.15K and moderate pressures. *J. Taiwan Inst. Chem. Eng.* **2013**, *44*, 879–885. [CrossRef]
28. Zhang, Y.; Ji, X.; Lu, X. Choline-based deep eutectic solvents for CO_2 separation: Review and thermodynamic analysis. *Renew. Sustain. Energy Rev.* **2018**, *97*, 436–455. [CrossRef]
29. Sarmad, S.; Xie, Y.; Mikkola, J.-P.; Ji, X. Screening of deep eutectic solvents (DESs) as green CO_2 sorbents: From solubility to viscosity. *New J. Chem.* **2017**, *41*, 290–301. [CrossRef]
30. Kumar, K.; Keshri, S.; Bharti, A.; Kumar, S.; Mogurampelly, S. Solubility of Gases in Choline Chloride-Based Deep Eutectic Solvents from Molecular Dynamics Simulation. *Ind. Eng. Chem. Res.* **2022**, *61*, 4659–4671. [CrossRef]
31. Ali, E.; Hadj-Kali, M.K.; Mulyono, S.; Alnashef, I. Analysis of operating conditions for CO_2 capturing process using deep eutectic solvents. *Int. J. Greenh. Gas Control* **2016**, *47*, 342–350. [CrossRef]
32. Cao, L.; Huang, J.; Zhang, X.; Zhang, S.; Gao, J.; Zeng, S. Imidazole tailored deep eutectic solvents for CO_2 capture enhanced by hydrogen bonds. *Phys. Chem. Chem. Phys.* **2015**, *17*, 27306–27316. [CrossRef] [PubMed]
33. Trivedi, T.J.; Lee, J.H.; Lee, H.J.; Jeong, Y.K.; Choi, J.W. Deep eutectic solvents as attractive media for CO_2 capture. *Green Chem.* **2016**, *18*, 2834–2842. [CrossRef]
34. Shukla, S.K.; Nikjoo, D.; Mikkola, J.-P. Is basicity the sole criterion for attaining high carbon dioxide capture in deep-eutectic solvents? *Phys. Chem. Chem. Phys.* **2020**, *22*, 966–970. [CrossRef]
35. Zhang, K.; Hou, Y.; Wang, Y.; Wang, K.; Ren, S.; Wu, W. Efficient and Reversible Absorption of CO_2 by Functional Deep Eutectic Solvents. *Energy Fuels* **2018**, *32*, 7727–7733. [CrossRef]

36. Gu, Y.; Hou, Y.; Ren, S.; Sun, Y.; Wu, W. Hydrophobic Functional Deep Eutectic Solvents Used for Efficient and Reversible Capture of CO_2. *ACS Omega* **2020**, *5*, 6809–6816. [CrossRef]
37. Qian, W.; Hao, J.; Zhu, M.; Sun, P.; Zhang, K.; Wang, X.; Xu, X. Development of green solvents for efficient post-combustion CO_2 capture with good regeneration performance. *J. CO_2 Util.* **2022**, *59*, 101955. [CrossRef]
38. Cui, G.; Lv, M.; Yang, D. Efficient CO_2 absorption by azolide-based deep eutectic solvents. *Chem. Commun.* **2019**, *55*, 1426–1429. [CrossRef]
39. Wang, Z.; Wu, C.; Wang, Z.; Zhang, S.; Yang, D. CO_2 capture by 1,2,3-triazole-based deep eutectic solvents: The unexpected role of hydrogen bonds. *Chem. Commun.* **2022**, *58*, 7376–7379. [CrossRef]
40. Lee, Y.-Y.; Penley, D.; Klemm, A.; Dean, W.; Gurkan, B. Deep Eutectic Solvent Formed by Imidazolium Cyanopyrrolide and Ethylene Glycol for Reactive CO_2 Separations. *ACS Sustain. Chem. Eng.* **2021**, *9*, 1090–1098. [CrossRef]
41. Wang, Z.; Wang, Z.; Chen, J.; Wu, C.; Yang, D. The Influence of Hydrogen Bond Donors on the CO_2 Absorption Mechanism by the Bio-Phenol-Based Deep Eutectic Solvents. *Molecules* **2021**, *26*, 7167. [CrossRef] [PubMed]
42. Yan, H.; Zhao, L.; Bai, Y.; Li, F.; Dong, H.; Wang, H.; Zhang, X.; Zeng, S. Superbase Ionic Liquid-Based Deep Eutectic Solvents for Improving CO_2 Absorption. *ACS Sustain. Chem. Eng.* **2020**, *8*, 2523–2530. [CrossRef]
43. Fu, H.; Wang, X.; Sang, H.; Liu, J.; Lin, X.; Zhang, L. Highly efficient absorption of carbon dioxide by EG-assisted DBU-based deep eutectic solvents. *J. CO_2 Util.* **2021**, *43*, 101372. [CrossRef]
44. Sang, H.; Su, L.; Han, W.; Si, F.; Yue, W.; Zhou, X.; Peng, Z.; Fu, H. Basicity-controlled DBN-based deep eutectic solvents for efficient carbon dioxide capture. *J. CO_2 Util.* **2022**, *65*, 102201. [CrossRef]
45. Wang, Z.; Wang, Z.; Huang, X.; Yang, D.; Wu, C.; Chen, J. Deep eutectic solvents composed of bio-phenol-derived superbase ionic liquids and ethylene glycol for CO_2 capture. *Chem. Commun.* **2022**, *58*, 2160–2163. [CrossRef]
46. Jiang, B.; Ma, J.; Yang, N.; Huang, Z.; Zhang, N.; Tantai, X.; Sun, Y.; Zhang, L. Superbase/Acylamido-Based Deep Eutectic Solvents for Multiple-Site Efficient CO_2 Absorption. *Energy Fuels* **2019**, *33*, 7569–7577. [CrossRef]
47. Wang, Z.; Chen, M.; Lu, B.; Zhang, S.; Yang, D. Effect of Hydrogen Bonds on CO_2 Capture by Functionalized Deep Eutectic Solvents Derived from 4-Fluorophenol. *ACS Sustain. Chem. Eng.* **2023**, *11*, 6272–6279. [CrossRef]
48. Zhang, N.; Huang, Z.; Zhang, H.; Ma, J.; Jiang, B.; Zhang, L. Highly Efficient and Reversible CO_2 Capture by Task-Specific Deep Eutectic Solvents. *Ind. Eng. Chem. Res.* **2019**, *58*, 13321–13329. [CrossRef]
49. Shukla, S.K.; Mikkola, J.-P. Intermolecular interactions upon carbon dioxide capture in deep-eutectic solvents. *Phys. Chem. Chem. Phys.* **2018**, *20*, 24591–24601. [CrossRef]
50. Klemm, A.; Vicchio, S.P.; Bhattacharjee, S.; Cagli, E.; Park, Y.; Zeeshan, M.; Dikki, R.; Liu, H.; Kidder, M.K.; Getman, R.B.; et al. Impact of Hydrogen Bonds on CO_2 Binding in Eutectic Solvents: An Experimental and Computational Study toward Sorbent Design for CO_2 Capture. *ACS Sustain. Chem. Eng.* **2023**, *11*, 3740–3749. [CrossRef]
51. Tan, Z.; Zhang, S.; Zhao, F.; Zhang, R.; Tang, F.; You, K.; Luo, H.A.; Zhang, X. SnO_2/ATP catalyst enabling energy-efficient and green amine-based CO_2 capture. *Chem. Eng. J.* **2023**, *453*, 139801. [CrossRef]
52. Zhang, X.; Zhang, S.; Tan, Z.; Zhao, S.; Peng, Y.; Xiang, C.; Zhao, W.; Zhang, R. One-step synthesis of efficient manganese-based oxide catalyst for ultra-rapid CO_2 absorption in MDEA solutions. *Chem. Eng. J.* **2023**, *465*, 142878. [CrossRef]
53. Zhang, X.; Zhang, S.; Tang, F.; Tan, Z.; Peng, Y.; Zhao, S.; Xiang, C.; Sun, H.; Zhao, F.; You, K.; et al. Solid base LDH-catalyzed ultrafast and efficient CO_2 absorption into a tertiary amine solution. *Chem. Eng. Sci.* **2023**, *278*, 118889. [CrossRef]